Bioelectromagnetics 33:298–308 (2012)

Effect of Static Magnetic Fields on the Growth, Photosynthesis and Ultrastructure of *Chlorella kessleri* Microalgae

Darcy P. Small,[1] Norman P.A. Hüner,[2,3] and Wankei Wan[1,4]*

[1]*Department of Chemical and Biochemical Engineering, University of Western Ontario, London, ON, Canada*
[2]*Department of Biology, University of Western Ontario, London, ON, Canada*
[3]*Biotron Experimental Climate Change Research Center, University of Western Ontario, London, ON, Canada*
[4]*University of Western Ontario, Graduate Program in Biomedical Engineering, London, ON, Canada*

Microalgal biotechnology could generate substantial amounts of biofuels with minimal environmental impact if the economics can be improved by increasing the rate of biomass production. *Chlorella kessleri* was grown in a small-scale raceway pond and in flask cultures with the entire volume, 1% (v/v) at any instant, periodically exposed to static magnetic fields to demonstrate increased biomass production and investigate physiological changes, respectively. The growth rate in flasks was maximal at a field strength of 10 mT, increasing from 0.39 ± 0.06 per day for the control to 0.88 ± 0.06 per day. In the raceway pond the 10 mT field increased the growth rate from 0.24 ± 0.03 to 0.45 ± 0.05 per day, final biomass from 0.88 ± 0.11 to 1.56 ± 0.18 g/L per day, and maximum biomass production from 0.11 ± 0.02 to 0.38 ± 0.04 g/L per day. Increased pigment, protein, Ca, and Zn content made the biomass produced with magnetic stimulation nutritionally superior. An increase in oxidative stress was measured indirectly as a decrease in antioxidant capacity from 26 ± 2 to 17 ± 1 μmol antioxidant/g biomass. Net photosynthetic capacity (NPC) and respiratory rate were increased by factors of 2.1 and 3.1, respectively. Loss of NPC enhancement after the removal of magnetic field fit a first-order model well ($R^2 = 0.99$) with a half-life of 3.3 days. Transmission electron microscopy showed enlarged chloroplasts and decreased thylakoid order with 10 mT treatment. By increasing daily biomass production about fourfold, 10 mT magnetic field exposure could make algal oil cost competitive with other biodiesel feedstocks. Bioelectromagnetics 33:298–308, 2012. © 2011 Wiley Periodicals, Inc.

Key words: oxidative stress; photosynthesis; microalgae; biofuel; nutrition

INTRODUCTION

Although the Earth's magnetic field intensity is about 0.05 mT, the static magnetic fields (SMF) near electrical devices can be much higher [Hashish et al., 2008]. Magnetic fields up to 2 mT have been measured on some rail systems; up to 5 mT during welding; up to 50 mT in accessible areas in power-plants; up to 100 mT in aluminum production facilities; and even higher for some high-tech and medical facilities [World Health Organization (WHO), 2006]. The biological and health effects of exposure to these elevated SMF intensities are often subjects of concern [Repacholi and Greenebaum, 1999]. In mammalian cells SMF of 10 mT or less have been shown to affect cell differentiation [Pagliara et al., 2005], morphology [Chionna et al., 2003], growth, size [Rosen and Chastney, 2009], and mitosis [Tenuzzo et al., 2006]. In rat and mouse models oxidative stress was increased by SMF [Amara et al., 2007] as was the rate of tumor development and growth [Chionna et al., 2003], which has led to the suggestion that SMF might promote cancer. SMF cause a variety of effects in microorganisms and plants such as changes in gene expression and growth in *E. coli*

Grant sponsors: Ontario Centers of Excellence; Natural Science and Engineering Research Council; University of Western Ontario.

*Correspondence to: Wankei Wan, Faculty of Engineering, Department of Chemical and Biochemical Engineering, University of Western Ontario, London, ON, Canada N6A 5B9.
E-mail: wkwan@eng.uwo.ca

Received for review 22 March 2011; Accepted 31 August 2011

DOI 10.1002/bem.20706
Published online 27 September 2011 in Wiley Online Library (wileyonlinelibrary.com).

[Potenza et al., 2004], increased seed germination, growth, and pigment content [Cakmak et al., 2010], and increased oxidative stress in plant cells [Sahebjamei et al., 2007]. Photosynthetic cells have been used as models of SMF-induced oxidative stress [Wang et al., 2008].

Because of their high photosynthetic efficiency (PE), ability to grow in saline or waste waters, high tolerance for CO_2 and their unique biochemical composition, microalgae are being investigated for biofuel production, carbon capture, and advanced nutrient production [Chisti, 2007; Stucki et al., 2009]. However, due to high production costs, implementation of microalgal biotechnology is currently limited to nutrients and high value products [Apt and Behrens, 1999; Williams and Laurens, 2010].

Many researchers are attempting to increase microalgal biomass production rates by developing closed photobioreactors (PBRs) [Chisti, 2007]. However, PBRs may cost ten times more than open systems [Mata et al., 2010], limiting them to higher value products, which are currently produced mainly in open ponds [Pulz and Gross, 2004], where PBRs are used to generate the pond inoculums. Growth medium formulation [Tran et al., 2010], high CO_2 levels [Papazi et al., 2008], high-frequency light/dark cycling [Grobbelaar et al., 1996], genetic engineering [Williams and Laurens, 2010], and exposure to SMF [Wang et al., 2008] have been proposed to increase biomass production.

In 1998, Hirano et al. measured the growth of the cyanobacterium *Spirulina platensis* with continuous SMF exposure and found that 10 mT SMF maximized growth and increased the chlorophyll (chl.) concentration and photosynthetic rate. Li et al. [2007] grew *S. platensis* in a small-scale airlift PBR with periodic exposure to a 250 mT SMF and found a 50% increase in biomass and changes in metal and amino acid content. Wang et al. [2008] studied the effect of SMF on the eukaryotic green microalga *Chlorella vulgaris* and found that 10 mT SMF maximized growth rate but increased oxidative stress.

Chlorella sp. is used to produce dried biomass and aqueous extracts, which show anti-cancer and anti-obesity effects and promote immune and cardiovascular health [Gantar and Svirĉev, 2008]. Since most microalgal biomass is produced in open systems [Pulz and Gross, 2004], we built a laboratory-scale raceway pond and exposed *Chlorella kessleri* to a uniform SMF to study the effect on growth under simulated industrial conditions, and grew axenic flask cultures to study changes in biochemical composition, photosynthesis, and cellular ultrastructure.

MATERIALS AND METHODS

Microalgal Strains, Growth Conditions, and SMF Exposure

C. kessleri (UTEX 398) was grown in 0.22 μm filter-sterilized BG-11 freshwater media modified by adding 5 mg/L Iron (III) ethylenediaminetetraacetic acid (EDTA), made with glass-distilled deionized water (DDIW). All chemicals were analytical grade and purchased from Sigma–Aldrich (St. Louis, MO). *C. kessleri* was grown in this media for 3 months for acclimation, and the inoculum was taken from cultures in the exponential growth phase.

Growth and biomass production were measured in a small-scale raceway pond made from ABS plastic, with an effective volume of 3.6 L. The pond features an oval channel with a usable depth of 6 cm and is circulated by a paddle wheel. Filter-sterilized (0.22 μm) air is bubbled into the reactor via four perforated stainless steel tubes to provide carbon dioxide (388 ppmv). A schematic generated using SolidWorks 2009 v. SP3.0 (Dassault Systèmes, Vélizy-Villacoublay, France) is shown in Figure 1.

The pond was operated in a biosafety cabinet to minimize contamination. DDIW was added daily to maintain constant volume. The aeration rate was 0.5 L air/min and the paddle wheel was set at 20 RPM, providing a surface velocity of about 25 cm/s. All experiments were run at 22 ± 1 °C. Artificial light was provided by a 1:1 mix of GE Ecolux (#80187, Foxboro, MA) and Philips Plant and Aquarium (#49893, Markham, ON, Canada) fluorescent tubes for 16 h each day. A Li-Cor LI190 quantum sensor (Lincoln, NE) was used to measure photosynthetically active radiation (PAR), which was set at 200 ± 10 μmol photons/m^2s. The pond was sterilized with 70% (v/v) aqueous isopropanol and washed with DDIW.

A side-stream from the reactor was exposed to a uniform 10 mT SMF generated by a water-cooled solenoid, which caused no measurable heating, facing magnetic North. Temporal and spatial homogeneity of the SMF were measured with a gauss meter (model 5180, Cole-Parmer, Vernon Hills, IL). When set at 10 mT the SMF measured at the solenoid center did not change by more than 0.1 mT. The solenoid inner diameter was 3 cm and only the innermost 1.5 cm of the air-space between the solenoid poles was used for SMF exposure. When the electromagnet was set at 10 mT the SMF intensity at the edges of this volume was over 9 mT. The side stream was run by a peristaltic pump at 200 ml/min, with 1% (v/v) of the reactor volume exposed at any time, so that the entire reactor

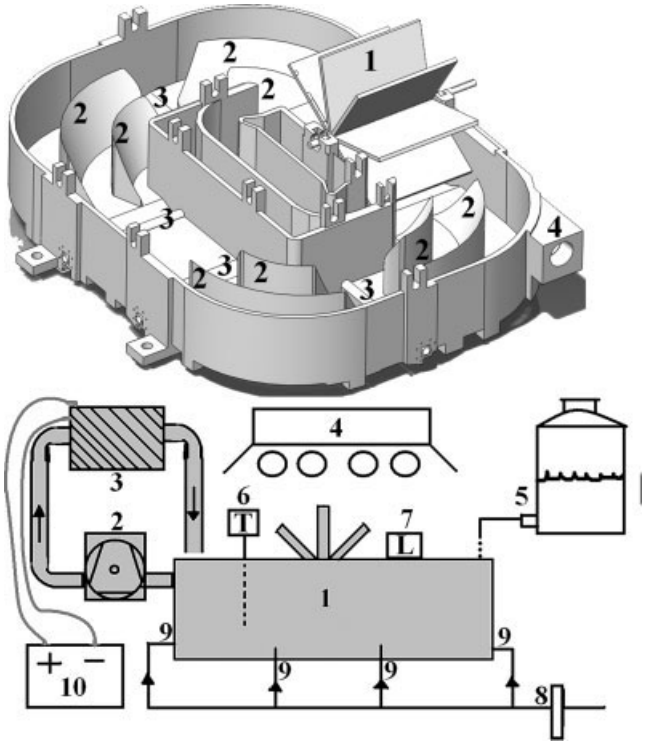

Fig. 1. **Top**: Raceway pond used as model for large-scale microalgal biomass production. 1: Paddle wheel; 2: baffles; 3: cylindrical aerators; 4: location of side-stream for magnetic field exposure. Length of the pond in the longest dimension is approximately 40 cm. **Bottom**: Schematic of experimental set-up. 1: Raceway pond; 2: peristaltic pump; 3: solenoid electromagnet; 4: array of fluorescent lights; 5: water to keep at constant level; 6: thermocouple; 7: quantum sensor; 8: filter-sterilized air source; 9: aerator discharge into raceway; 10: DC power supply. Raceway pond was used to determine growth curves under the Earth's magnetic field (control) and 10 mT magnetic field strength, while a similar set-up except with growth in axenic Erlenmeyer flasks was used for other experiments.

contents were moved through the electromagnet about every 18 min. As a control the same set-up was used with the electromagnet shut off. A 15% (v/v) inoculum from axenic flasks was used to give an initial cell concentration between 10 and 25 $\times$ 10^6 cells/ml.

Axenic cultures were also grown in 2 L Erlenmeyer flasks with the same culture and SMF exposure parameters, except with mixing by delivering 0.2 vvm air and SMF intensities of 0 (control), 5, 10, and 15 mT, to determine the optimal SMF strength and the physiological effects of SMF without the effects of contamination. For flask cultures, silicone rubber tubing was inserted into the flask stoppers for peristaltic pumping through the electromagnet. The flasks and the entire silicone rubber tubing assembly were autoclaved for sterilization. All experiments and analytical techniques were repeated in triplicate, unless otherwise noted.

Biomass Determination, Monitoring of Contamination, and Growth Quantification

Samples were removed aseptically for biomass determination by measuring turbidity at 750 nm, which correlated well with gravimetrically measured biomass for samples exposed to the same SMF ($R^2 = 0.99$), using an ultraviolet–visible (UV–Vis) spectrophotometer (DU-520, Beckman-Coulter, Brea, CA). Biomass was also estimated with a hemocytometer (Brightline 3100, Hausser Scientific, Horsham, PA), using 20 0.0025 mm^2 squares, which correlated well with gravimetric measurements at the same SMF ($R^2 = 0.98$). The average biomass between the two methods is reported. Final biomass concentration was measured gravimetrically after washing with DDIW and lyophilizing.

Each day a 10 μl inoculating loop was used to streak three Petri dishes of Difco nutrient agar (#212000, BD Difco, Sparks, MD), which were incubated at 25 °C before counting colonies. Purity was also measured as the ratio of absorbance at the chl. peak (680 nm) to turbidity (750 nm).

The growth rate, μ, was calculated daily using the measured biomass concentration, C_{bm}:

$$\mu = \frac{\ln(C_{bm2}) - \ln(C_{bm1})}{t_2 - t_1} \quad (1)$$

where t is time, and the subscripts 1 and 2 denote the initial and next measurements, respectively.

The daily production rate, P, was calculated from the following equation:

$$P = C_{bm}\mu \quad (2)$$

Biochemical Analysis

Biochemical composition was determined using biomass produced in axenic flask cultures harvested at the beginning of the stationary phase of growth. Ash content was determined gravimetrically by burning oven-dried samples at 550 °C for 4 h. Carbohydrates were extracted by sonication of lyophilized samples for 5 min at 60 W using a Misonix XL-2000 sonication probe (Newtown, CT) in 1 M acetic acid [Mecozzi et al., 2000]. The supernatant was subjected to the phenol sulphuric acid method using glucose as a standard [DuBois et al., 1956]. Proteins were extracted by sonication for 3 min at 60 W in 1% (w/v) sodium dodecyl sulphate [Meijer and Wijfels, 1998]. The supernatant was diluted 10 times

and proteins were quantified using the Bradford method, with bovine serum albumin as a standard (#500, Bio-Rad, Hercules, CA). Lipid content was determined gravimetrically by sonication of the lyophilized biomass for 3 min at 60 W in 2:1 (v/v) chloroform/methanol and then by Soxhlet extraction [Folch et al., 1957]. Pigments were extracted by sonication in 80% (v/v) aqueous acetone. Chlorophyll a, chlorophyll b, and total carotenoid concentration were determined by UV–Vis spectrometry from absorbance at 663, 645, and 480 nm [Arnon, 1949; Kirk and Allen, 1965]. Antioxidants were extracted from sonicated cells using 50% (v/v) aqueous ethanol and quantified using the 2,2-diphenyl-1-picrylhydrazyl (DPPH) method [Wang et al., 2008]. Metal content was determined with nitric acid digestion followed by atomic absorption spectroscopy (SpectrAA-55, Varian, Cary, NC) [Al-Homaidan, 2006]. Fatty acid composition was determined using gas chromatography (GC) as previously described [Metherel et al., 2009].

Effect of 10 mT SMF on Photosynthesis and Ultrastructure

Axenic flask cultures were used to study photosynthesis. The rate of respiration and photosynthetic oxygen evolution were measured using an oxygen electrode chamber illuminated with red (650 nm) light-emitting diodes (LEDs; Oxylab LD2/3, Hansatech Instruments, Norfolk, UK). The decay of the SMF effect was measured by comparing oxygen production of 5-day-old control and 10 mT cultures, with the SMF removed after the first measurement.

The ultrastructure cells from axenic flask cultures in the exponential growth phase exposed to SMF were investigated using transmission electron microscopy (TEM). Cells were fixed with 2% (v/v) glutaraldehyde and then stained with 1% (w/v) osmium tetroxide in sodium cacodylate buffer (0.1 M) for 1 h. The cells were dehydrated by exchange with ethanol (25%, 50%, 75%, and 100%, v/v $\times$ 3) and embedded in London Resin (LR) White hard acrylic resin (L9774, Sigma–Aldrich). The embedded samples were ultrathin sectioned ($\sim$70 nm) using a Reichert Ultracut E ultramicrotome (#701701, Buffalo, NY) and collected on Formvar carbon-coated 100 mesh copper grids (FCF100-Cu, Electron Microscopy Sciences, Hatfield, PA). Post-staining was done with 5% (w/v) uranyl acetate and 2% (w/v) lead citrate for 5 min and 4 min, respectively. Imaging was conducted using a Philips CM-10 transmission electron microscope (New York, NY) set at an accelerating voltage of 80 kV with images captured using a Hamamatsu digital camera (C9100-03, Bridgewater, NJ). Cell size was measured by forward scattering using a flow cytometer (FACS-Calibur 643271, Becton-Dickinson, Pasadena, CA) with 6 μm latex beads as an internal standard, and data were normalized using bead forward scattering. Cell feature areas ($n = 20$) were determined manually using ImageJ software (1.43 U Java 1.6.0_10 32 bit, Wayne Rasband, National Institutes of Health, Bethesda, MD).

All statistical analyses were performed using SigmaStat 3.5 for Windows (Systat Software, San Jose, CA). Mean values were compared using the two-tailed Student's *t*-test. A *P*-value of 0.05 or less was considered significant, and results are reported as the mean $\pm$ 1 standard error.

RESULTS

Effect of 10 mT SMF on Growth in Axenic Flask Cultures and Raceway Ponds

The optimum SMF for maximum specific growth rate (μ) during the exponential growth phase, calculated according to Equation (1), was determined to be 10 mT using axenic flask cultures with 0, 5, 10, and 15 mT SMF. A 10 mT SMF more than doubled the growth rate compared to the sham control (Fig. 2). Therefore, cells were grown in a small-scale raceway pond with periodic exposure to a 10 mT SMF. Growth curves for control and 10 mT SMF-treated cultures are shown in Figure 3. Normalized biomass, calculated as biomass density divided by initial biomass density, was significantly higher for treated cells after just 2 days of growth, at 1.16 ± 0.03 for the control and 1.30 ± 0.04 for the 10 mT treatment. The total C_{bm} at the end of each run was measured directly. As shown in Figure 4,

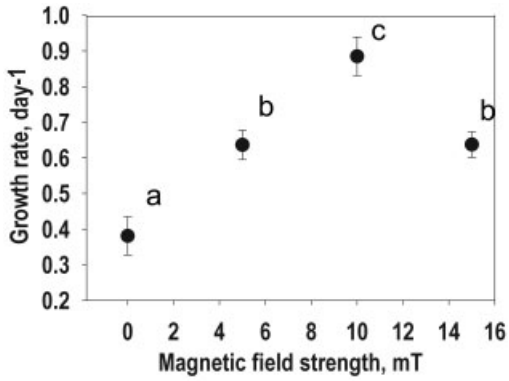

Fig. 2. Optimum magnetic field strength for maximum growth rate (μ) of *C. kessleri*. The data points shown (a, b, c, d) are statistically different from each other ($P = 0.05$, $n = 3$). Mean $\pm$ 1 standard error is shown.

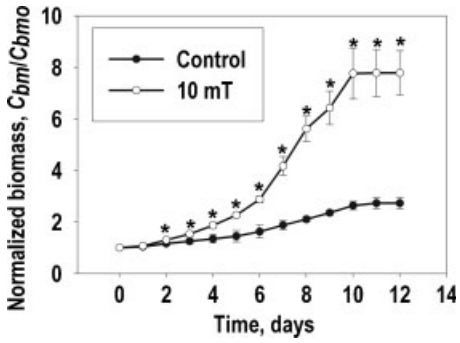

Fig. 3. Normalized biomass versus time for *C. kessleri* cells exposed to 10 mT magnetic field and cells exposed only to Earth's magnetic field in the raceway pond (control). The initial biomass concentration was 0.32 ± 0.07 for the control treatment and 0.22 ± 0.06 g/L for the 10 mT treatment. Points significantly different from the control are marked with an asterisk ($P \leq 0.05$, $n = 3$). Mean ± 1 standard error is shown.

the final C_{bm} was 0.88 ± 0.11 g/L for the control and significantly higher for the 10 mT treatment (1.56 ± 0.18 g/L). The maximum growth rate was significantly higher for the 10 mT treatment and persisted to higher biomass concentrations, leading to a fourfold increase in daily biomass production (Fig. 4, third column).

Contamination was monitored in raceway pond experiments to ensure that the observed effects were caused by SMF treatment and not by contamination. The control treatment had 14.8 ± 2.2 colonies per Petri dish at the end of the run, not significantly different from the 15.6 ± 2.5 colonies per Petri dish for the 10 mT treatment. All colonies were an opaque, shiny, cream color with a rugose surface. The final ratio of chlorophyll absorbance to turbidity

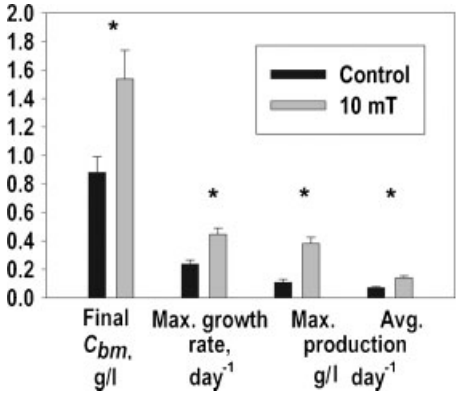

Fig. 4. Final biomass, maximum growth rate, maximum daily production rate, and average daily production rate are all significantly higher for the 10 mT treatment, compared to the control. *C. kessleri* cells were grown in the raceway pond. Statistically significant differences from the control are marked with an asterisk ($P \leq 0.05$, $n = 3$). Mean ± 1 standard error is shown.

was 1.94 ± 0.03 for the control and 1.93 ± 0.04 for the 10 mT treatment, with no significant difference in the growth rate between the two treatments.

Effect of 10 mT SMF on Biochemical Composition, Photosynthesis, and Cell Ultrastructure

As shown in Table 1, 10 mT SMF treatment led to significant increases in carbohydrate, protein, chl. a, and chl. b contents, which decreased the calculated calorific value of the biomass from 21 ± 1 to 20 ± 1 kJ/g. As shown in Table 2, SMF treatment increased the concentrations of Ca, Mn, Zn, and Ni, decreased Fe and Cu concentrations, and did not affect Mg concentration. Fatty acid composition was largely unaffected by SMF treatment (Table 3). The rare fatty acids 15:0 and 18:1 n-7 significantly increased with SMF treatment. The following non-abundant fatty acids were also measured with no significant change (data not shown): 12:0, 13:0, 14:0, 17:0, 18:0, 20:0, 22:0, 23:0, 24:0, 12:1, 14:1, 14:1trans, 15:1, 16:1, 20:1n-9, 22:1n-9, 24:1n-9, 18:3n-6, 20:2n-6, 20:3n-6, 20:4n-6, 22:2n-6, 22:4n-6, 22:5n-6, 20:3n-3, 20:5n-3, 22:5n-3, and 22:6n-3.

TABLE 1. Biomass and Pigment Composition for Control and 10 mT *C. kessleri* Cells

Component (%, w/w)	Control	10 mT
Carbohydrate	38.9 ± 0.7*	42.2 ± 0.7
Protein	29.7 ± 0.6*	32.3 ± 0.6
Lipid	24.5 ± 1.3	20.3 ± 1.1
Ash	6.9 ± 1.1	5.2 ± 1.3
Chlorophyll a	2.5 ± 0.1*	2.88 ± 0.09
Chlorophyll b	0.53 ± 0.06*	0.87 ± 0.04
Carotenoids	0.07 ± 0.02	0.08 ± 0.02
Antioxidants[a]	26 ± 2*	17 ± 1

Statistically significant differences are marked with an asterisk ($P \leq 0.05$, $n = 3$). Mean ± 1 standard error is shown.
[a]μmol antioxidant/g biomass.

TABLE 2. Metal Content of *C. kessleri* Cells Subjected to Control and 10 mT Treatments

Metal content (mg/kg)	Control	10 mT
Mg	3370 ± 50	3360 ± 40
Ca	1440 ± 30*	3110 ± 50
Fe	1980 ± 40*	1300 ± 50
Zn	41 ± 1*	88 ± 2
Mn	25 ± 1*	47 ± 1
Cu	28.4 ± 0.8*	20 ± 1
Ni	1.2 ± 0.1*	4.1 ± 0.5

Statistically significant differences are marked with an asterisk ($P \leq 0.05$, $n = 3$). Mean ± 1 standard error is shown.

TABLE 3. Changes in Fatty Acid Composition With 10 mT Magnetic Field Exposure of *C. kessleri*

(%, w/w of fatty acids)		
Name	Control	10 mT
SFAs	20.5 ± 0.3	20.7 ± 0.5
16:0	16.2 ± 0.3	16.4 ± 0.4
15:0	0.198 ± 0.004*	0.238 ± 0.006
MUFAs	15.0 ± 0.2	14.6 ± 0.3
17:1	9.5 ± 0.2	9.1 ± 0.2
18:1n-9	3.57 ± 0.07	3.42 ± 0.07
18:1n-7	0.44 ± 0.01*	0.62 ± 0.01
N-6	23.7 ± 0.4	23.0 ± 0.5
18:2n-6	23.2 ± 0.4	22.6 ± 0.5
N-3	40.9 ± 0.6	41.6 ± 0.8
18:3n-3	40.8 ± 0.6	41.5 ± 0.8

SFA, saturated fatty acid; MUFA, monounsaturated fatty acid; N-6, omega-6 fatty acid; N-3, omega-3 fatty acid.
Only major fatty acids of each category and fatty acids with statistically significant changes are shown.
Statistically significant differences are marked with an asterisk ($P \leq 0.05$, $n = 3$). Mean ± 1 standard error is shown.

All photosynthetic parameter measurements increased with 10 mT SMF treatment (Table 4, Fig. 5). Using the measured extinction coefficient at 650 nm, the maximum moles of O_2 evolved per photon absorbed was calculated to be 45.7%, the theoretical limit of 1/8 for 10 mT SMF-treated cells [Huner et al., 2003]. The effect of SMF on net photosynthetic capacity (NPC) persisted for at least 5 days (Fig. 6). The decline in relative NPC fits a first-order kinetic model well ($R^2 = 0.99$):

$$\frac{R_{\max}}{R_{\max(\text{control})}} = 1 + 0.74e^{-0.21t} \quad (3)$$

where $R_{\max}$ is the NPC of 10 mT SMF-treated cells, $R_{\max(\text{control})}$ is the NPC of the control cells, and t is the time (in days) after the cessation of SMF treatment. The relative NPC increase from SMF treatment fell toward the control NPC with a half-life of 3.3 days.

SMF exposure increased chloroplast and thylakoid area but thylakoids became disorganized, with the more abundant chloroplast starch granules interrupting stacked thylakoids (Fig. 7, Table 5). Total starch area and pyrenoid center area seemed to increase but the change was not statistically significant. The mean forward scattering for control and 10 mT SMF-treated cells was 414 ± 3 and 315 ± 2 AU, respectively, indicating a decrease in cell size with SMF exposure. This was also supported by comparison of cell count to dry weight, which revealed that control cells were significantly heavier (12.2 ± 0.3 pg/cell) than 10 mT cells (8.9 ± 0.3 pg/cell). Antioxidant content decreased significantly with SMF treatment from 26 ± 2 to 17 ± 1 μmol/g biomass (Table 1).

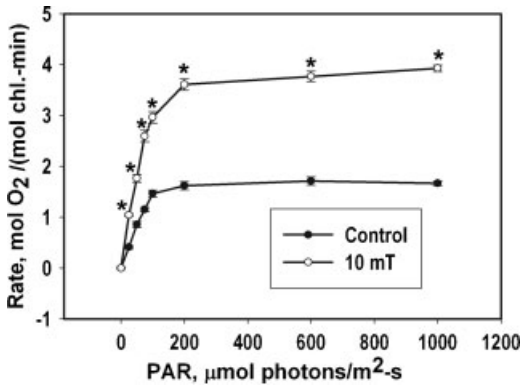

Fig. 5. Photosynthetic light response curves for *C. kessleri* cells on a total chlorophyll basis. Statistically significant differences from the control are marked with an asterisk ($P \leq 0.05$, $n = 3$). Mean ± 1 standard error is shown.

DISCUSSION

From the results of this study it is clear that mT-range intensity SMF have a significant effect on the growth of *C. kessleri* (Fig. 2). Hirano et al. [1998] and Wang et al. [2008] also found growth enhancement of *S. platensis* and *C. vulgaris* treated with mT-range intensity SMF. This suggests that SMF exposure might enhance the growth of many species of microalgae and cyanobacteria, although a broader study of the effect of SMF on the growth of many genera of microalgae and cyanobacteria is

TABLE 4. Effect of 10 mT Magnetic Field Treatment on Photosynthesis in *C. kessleri* Measured With an Oxygen Electrode

Photosynthetic parameter	Unit	Control	10 mT
Respiration	mol O_2/mol chl-min	−0.30 ± 0.03	−0.94 ± 0.03
Gross photosynthetic capacity	mol O_2/mol chl-min	1.72 ± 0.08	3.93 ± 0.07
Net photosynthetic capacity	mol O_2/mol chl-min	1.42 ± 0.08	2.99 ± 0.07
Maximum photosynthetic efficiency	mol O_2/mol photons	0.028 ± 0.001	0.057 ± 0.001
Maximum photosynthetic efficiency	%	22 ± 1	46 ± 1

All values are significantly different between treatments ($P \leq 0.05$, $n = 3$). Mean ± 1 standard error is shown.

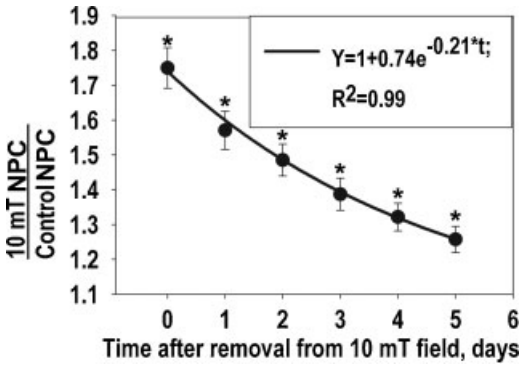

Fig. 6. Decline in magnetic field effect on net photosynthetic capacity (NPC) for *C. kessleri* cells exposed to 10 mT magnetic field treatment for 5 days and then grown under only the Earth's magnetic field for 5 days. Treated cells were removed from the magnetic field at day 0, and control cells were grown identically but exposed only to Earth's magnetic field. The *y*-axis shows net photosynthetic capacity of treated cells divided by the capacity of control cells, per mol of chlorophyll. Data is fit with an exponential curve showing first-order loss of the magnetic field effect ($R^2 = 0.99$). Points with statistically significant difference from the control are marked with an asterisk ($P \leq 0.05$, $n = 3$). Mean $\pm$ 1 standard error is shown.

needed. The growth of *C. kessleri* reached a maximum with 10 mT SMF exposure (Fig. 2). A maximum growth rate was also found at an SMF intensity of about 10 mT in *S. platensis* and *C. vulgaris* [Hirano et al., 1998; Wang et al., 2008]. Li et al. [2007] found that *S. platensis* biomass production was maximal with 0.25 T SMF but they did not investigate SMF below 0.1 T intensity. It is unclear why the growth rate reached a maximum at 10 mT, a strong SMF compared to the Earth's SMF ($\sim$50 μT), or why the SMF dose–response curve has a clear maximum at all (Fig. 2). Hirano et al. [1998] found control-level growth rates of *S. platensis* with 35 and 40 mT SMF and found significant growth retardation at 70 mT, while Wang et al. [2008] measured growth rates of *C. vulgaris* with SMF exposure up to 50 mT and found they fell back to control values above 35 mT. The SMF intensity dose–response curves presented in this study (Fig. 2) and by Hirano et al. [1998] and Wang et al. [2008] match each other closely and have the shape expected for a hormetic response to SMF strength [Allen et al., 2010; Woo and Shadel, 2011].

Exposure to a 10 mT SMF almost doubled the growth rate of *C. kessleri* grown in a raceway pond (Figs. 3 and 4). Since contamination levels were similar for control and SMF-exposed cultures, the increase in growth with SMF exposure is most likely unrelated to the low level of bacterial contamination. Furthermore, the increase in growth rates with

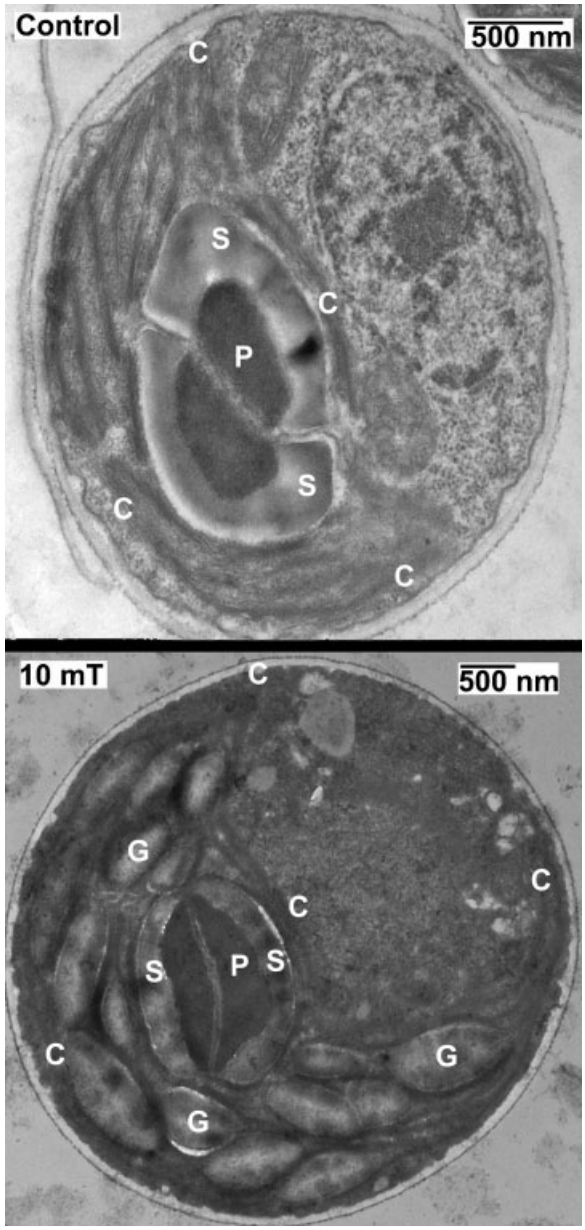

Fig. 7. TEM images of typical control cells exposed only to Earth's magnetic field (**top**) and 10 mT (**bottom**). Magnetized cells have a larger chloroplast with many starch granules while in the control cells, starch tends to be more concentrated at the pyrenoid. C: Chloroplast, four corners of cup-shaped organelle marked; P: pyrenoid center; S: pyrenoid starch plate; G: chloroplast starch granule (not all marked).

10 mT SMF exposure in the raceway pond was about the same as in axenic flask cultures (Fig. 2). Wang et al. [2008] reported a similar maximum increase in growth rates of about 60% with a 10 mT SMF in *C. vulgaris*. The growth curves were of sigmoidal shape with a higher growth rate in the exponential phase and higher C_{bm} at the onset of the stationary

TABLE 5. Changes in Ultrastructure of *C. kessleri* Cells Exposed to a 10 mT Magnetic Field

% Cell area/number per cell	Control	10 mT
Chloroplast area	45 ± 3*	59 ± 2
Pyrenoid area	11 ± 1.5	8 ± 1
Pyrenoid center area	3.6 ± 0.6	4.3 ± 0.6
Chloroplast starch granule area	4.4 ± 0.8*	10.9 ± 0.6
Pyrenoid starch area	7.8 ± 1.0*	3.6 ± 0.5
Total starch area	12 ± 1	14.6 ± 0.8
Thylakoid area	29 ± 2*	41 ± 1
Starch area/granule	0.9 ± 0.1	0.87 ± 0.04
Starch granule number	4.6 ± 0.5*	12.7 ± 0.7
Max. thylakoid stacking	7.8 ± 0.5*	5.2 ± 0.3

Statistically significant differences are marked with an asterisk ($P \leq 0.05$, $n = 20$). Mean ± 1 standard error is shown.

phase for 10 mT SMF-exposed cultures (Figs. 3 and 4). Overall, this resulted in about a fourfold increase in the maximum biomass production (Fig. 4). Li et al. [2007] also achieved a higher final C_{bm} in SMF-exposed cultures of *S. platensis*. Since mT-range intensity SMF exposure could be implemented inexpensively using permanent magnets (with the projected fourfold increase in biomass production), this approach could reduce the cost of algal oil production from about $1.80/L to about $0.45/L, below the cost of palm oil, neglecting the cost of downstream processing and assuming the same increase in productivity at a larger scale [Chisti, 2007]. The increased biomass production with SMF treatment in both axenic flask cultures and open raceway cultures implies that SMF treatment might increase biomass production in both PBRs and open ponds.

As shown in Tables 1 and 2, SMF of 10 mT increased the carbohydrate, protein, pigment, Ca, and Zn contents of the *C. kessleri* biomass, making it more nutritional. The lipids were rich in omega-3 fatty acids regardless of SMF treatment (Table 3). Wang et al. [2007] also observed an increased carbohydrate content with 10 mT SMF treatment of *C. vulgaris*. Hirano et al. [1998] found significant increases in pigment and carbohydrate concentration in *S. platensis* with 10 mT SMF treatment. Li et al. [2007] also measured an increase in protein content in *S. platensis* exposed to SMF. Lipid content decreased slightly but not statistically significant with SMF exposure, slightly decreasing the calorific value of the biomass, calculated to be 21 ± 1 and 20 ± 1 kJ/g for control and SMF-exposed cells, respectively; however, production of chemical energy increased overall due to increased biomass production. Fe and Ni, the two ferromagnetic metals measured in the biomass, decreased and increased in concentration, respectively, disfavoring the explanation that they were accelerated into the cells by the SMF. The content of Ca and Zn increased with SMF exposure, increasing the nutritional value of the biomass. Li et al. [2007] also found increased Ca concentration after SMF exposure of *S. platensis*. Since Wang et al. [2008] proposed *C. vulgaris* as a general model organism for SMF-induced oxidative stress it may be useful to compare our results to those obtained with SMF-treated non-photosynthetic organisms. Chionna et al. [2003] and Rosen and Chastney [2009] also observed increases in Ca concentration in SMF-exposed mammalian cells.

At the experimental light level of 200 μmol photons/m^2s, the net photosynthetic rate was about doubled by 10 mT SMF exposure allowing for the observed increase in the rate of photosynthetic chemical energy production (Fig. 5, Table 4). The respiration rate, NPC and growth rate of cells grown at 10 mT SMF were about 3, 2, and 2 times the rates for control cells, respectively. Since the increase in the growth rate was about equal to the increase in the photosynthetic rate, it should be possible to maintain photostasis without synthesizing more storage products [Ensminger et al., 2006]. We saw no significant change in total lipid content and only an 8% increase in carbohydrate content with SMF treatment (Table 1). The increase in photosynthetic parameters was several times higher than the increase in total chl. content, which increased by <30% with 10 mT SMF treatment (Table 1). The 50% higher increase in respiration rate than growth rate could be due to an increased need for nicotinamide adenine dinucleotide phosphate (NAD(P)H) to reduce nitrate for the increased protein content (Table 1). Grobbelaar et al. [1996] observed similar increases in NPC and chl. when high-frequency light/dark cycles were used to increase biomass production of *Scenedesmus obliquus*, and attributed the increased production to changes in photoacclimation.

The increase in NPC persisted for at least 5 days after removal of the 10 mT SMF (Fig. 6). Wang et al. [2008] measured growth after SMF exposure in a non-magnetized vessel over 3 days and still observed a significant increase of about 60% in the growth rate, compared to about 100% in this study (Fig. 3). The value reported by Wang et al. [2008] may be lower than in this study because the effect of SMF on NPC declined significantly by about 40% over 3 days (Fig. 6). The persistence of the SMF effect on photosynthesis and growth observed in this study suggests that SMF changes microalgal physiology rather than directly influencing photosynthesis;

otherwise, exposure of only 1% of the culture under reduced light would not be expected to increase growth efficiently with an effect persisting for days. Rosen and Chastney [2009] also observed long-term changes in mammalian cells exposed to SMF. The observed first-order decline of the SMF effect measured in this study (Fig. 6) could be due to the first-order degradation of some component, such as a protein or messenger ribonucleic acid (mRNA), whose degradation might be responsible for the loss of the SMF effect. Chloroplast mRNAs have relatively long half-lives that can be on the order of days [Monde et al., 2000].

The observed increase in chloroplast and thylakoid areas with 10 mT SMF exposure (Fig. 7, Table 5) helps explain the observed increase in photosynthesis with 10 mT SMF exposure (Fig. 5, Table 4). Similar to our observations, Wang et al. [2007] also observed a thylakoid disorder in SMF-treated *C. vulgaris* cells, which also had an increased growth rate. The increase in the pyrenoid core area was large but not statistically significant, although a large standard error was inherent in this measurement because the pyrenoid was not visible in many ultra-thin sections. Chankova et al. [1990] found enlargement of the pyrenoid in *C. vulgaris* after exposure to oxidative stress-inducing ionizing radiation. An increased pyrenoid core area could also help explain the increased rate of photosynthesis since the pyrenoid core usually contains enzymes such as carbonic anhydrase, which increases the local CO_2 concentration, and ribulose-1,5-bisphosphate carboxylase oxygenase, which catalyzes the first step of CO_2 fixation. The measured increase in carbohydrate content (Table 1) was supported by TEM observations of an increased plastid starch granule area (Fig. 7, Table 5). Larger changes in fatty acid composition (Table 3) might be expected with dramatic chloroplast enlargement; however, others did not observe changes in fatty acid composition with changes in chloroplast size [El-Sheekh and Fathy, 2009]. The increased number of starch granules and the decreased thickness of the pyrenoid starch plate suggest that cleavage of the starch plate is accelerated by SMF treatment since chloroplast starch granules are formed by cleavage of the pyrenoid starch plate [Griffiths, 1970]. Cell size decreased with 10 mT SMF, suggesting that division of both the organism and the starch plate were stimulated by 10 mT SMF, consistent with observations of increased mitosis under SMF by Levin and Ernst [1995] in sea urchins and Tenuzzo et al. [2006] in mammalian cells. Rosen and Chastney [2009] and Chionna et al. [2003] also observed changes in cell size and morphology in SMF-exposed mammalian cells.

Wang et al. [2008] argued that oxidative stress increased with increasing SMF, showing increased antioxidant enzyme activity, $^{\cdot}OH$ concentration and lipid peroxidation, and decreased antioxidant concentration. Similarly, we observed a decrease in antioxidant content by the DPPH method for 10 mT-exposed cultures. The growth rate was increased despite increased oxidative stress with 10 mT SMF, which suggests that the growth of *Chlorella* sp. is not limited by oxidative stress under the relatively low-light conditions used in this study and the study by Wang et al. [2008]. Wang et al. [2008] found that the increase in lipid peroxidation became significant at 45 mT SMF, after which the growth rate fell back to control values, which strongly supports the idea that growth retardation at stronger SMF is caused by increased oxidative stress.

It is has been shown that spin-correlated free radicals can be stabilized by mT-strength SMF [Galland and Pazur, 2005; Engström, 2006]. Therefore, one possible way that SMF could affect microalgal growth is by changing the concentrations of free radicals or the rates of reactions involving free radicals. Since Hirano et al. [1998] did not find any changes for heterotrophically grown cells it is likely that the SMF acts on the chloroplast. The effect of SMF on free radical concentration is amplified if the radical pair is oppositely charged and physically confined [Engström, 2006]. This is the case for the geminate products of photochemical charge separation, $P680^{+}/A_{II}^{-}$ (photosystem II primary donor/acceptor pair) and $P700^{+}/A_{I}^{-}$ (photosystem I primary donor/acceptor pair) [Zech et al., 1997], and therefore these radicals are some of the many possible sites of action for SMF exposure. Because of the observations suggesting increased oxidative stress in this study and the study by Wang et al. [2008], the free-radical effect appears to be the most likely mechanism for the effect of SMF on microalgae. The dose–response curves presented in this study (Fig. 2) and the studies by Hirano et al. [1998] and Wang et al. [2008] match the expected shape for a hormetic effect, and the onset of growth retardation is at the same SMF intensity as the onset of reactive oxygen species (ROS)-induced damage to lipids. This could suggest that the effect on growth is a hormetic response to SMF-stimulated ROS production; however, it is entirely unclear how increased ROS could lead to an increase in growth rate. It is also possible that the increased ROS production is only one effect of SMF exposure and that some other unrelated mechanism is responsible for the increase in growth rate, with

SMF-stimulated ROS production only responsible for the decline in growth at higher SMF strengths. Further experimentation is needed to determine more directly if SMF exposure affects free radical concentration in microalgae and how, if at all, this might be connected to increased growth. It has been suggested that increased longevity in *C. elegans* fed an oxidative stress-inducing modified diet is a hormetic response to oxidative stress [Woo and Shadel, 2011]. If further experiments can verify that the increase in growth with SMF exposure is caused by increased oxidative stress then this would be one of very few examples of a beneficial effect of oxidative stress, which would have major implications for aging research [Woo and Shadel, 2011] and biology, in general.

CONCLUSION

SMF exposure of *C. kessleri* almost quadrupled the biomass and lipid production rate in raceway ponds, making algal oil cost competitive with palm oil and therefore an economical biodiesel feedstock [Chisti, 2007]. SMF exposure also increased the nutritional value of the biomass by increasing protein, pigment, Ca, and Zn contents. Therefore, 10 mT SMF exposure could enhance production of *C. kessleri* biomass for biodiesel and nutritional products, or for the extraction of both types of products. Changes in biochemical composition, photosynthesis, and ultrastructure were observed. Given the many similarities between the results presented in this study and the results found by others for mammalian cells [Chionna et al., 2003; Rosen and Chastney, 2009] *Chlorella* sp. may be an appropriate model organism to study some aspects of SMF-induced changes in cell physiology. The decrease in cell size and changes in chloroplast organization suggest that SMF promotes mitosis and reorganization of organelles, both processes controlled by the cytoskeleton, which may also have implications for human health since SMF of about 10 mT are often encountered around electrical devices [Hashish et al., 2008]. The results suggested that SMF treatment affected the microalgae by changing free-radical concentrations. However, further investigation of the effects of SMF on free radical and ROS levels in microalgae is needed.

ACKNOWLEDGMENTS

The authors would like to acknowledge Ian Power and Gordon Southam for their help preparing samples for TEM, Ameer Taha, and Certo Extractions for fatty acid quantification, Charles G. Trick and Katrina Iglic for their help with flow cytometry, and Kenneth Wong for supplying and testing the electromagnet used in this study. DPS is the recipient of an Ontario Graduate Scholarship and a Canada Graduate Scholarship.

REFERENCES

Al-Homaidan AA. 2006. Heavy metal levels in Saudi Arabian *Spirulina*. Pak J Bio Sci 9:2693–2695.

Allen AK, Donato J, Wang HH, Cloud-Hansen KA, Davies J, Handelsman J. 2010. Call of the wild: Antibiotic resistance genes in natural environments. Nat Rev Microbiol 8:251–259.

Amara S, Abdelmelek H, Garrel C, Guiraud P, Douki T, Ravanat J-L, Favier A, Sakly M, Rhouma BK. 2007. Zinc supplementation ameliorates static magnetic field-induced oxidative stress in rat tissues. Enviro Toxicol Pharma 23:193–197.

Apt KE, Behrens PW. 1999. Commercial developments in microalgal biotechnology. J Phycol 35:215–236.

Arnon DI. 1949. Copper enzymes in isolated chloroplasts. Polyphenol oxidase in Beta vulgaris L. Plant Physiol 24:1–15.

Cakmak T, Dumlupinar R, Erdal S. 2010. Acceleration of germination and early growth of wheat and bean seedlings grown under various magnetic field and osmotic conditions. Bioelectromagnetics 31:120–129.

Chankova SG, Vinarova KM, Nikolov SH, Mehandjiev AD, Sergeeva SA, Ptitzina SN, Semov AB, Shevchenko VA. 1990. Changes in *Chlorella vulgaris B*. populations after chronic influence with chemical and physical mutagenic factors. Biol Plantarum 32:35–41.

Chionna A, Dwikit M, Panzarini E, Tenuzzo B, Carla EC, Verri T, Pagliara P, Abbro L, Dini L. 2003. Cell shape and plasma membrane alterations after static magnetic fields exposure. Eur J Histochem 47:299–308.

Chisti Y. 2007. Biodiesel from microalgae. Biotechnol Adv 24:294–306.

DuBois M, Gilles KA, Hamilton JK, Rebers PA, Smith F. 1956. Colorimetric method for determination of sugars and related substances. Anal Chem 28:350–356.

El-Sheekh MM, Fathy AA. 2009. Variation of some nutritional constituents and fatty acid profiles of *Chlorella vulgaris* Beijerinck grown under auto and heterotrophic conditions. Int J Bot 5:153–159.

Engström S. 2006. Magnetic field effects on free radical reactions in biology. In: Barnes FS, Greenebaum B, editors. Bioengineering and biophysical aspects of electromagnetic fields, 3rd edition. New York: CRC Press. pp 156–165.

Ensminger I, Florian B, Huner NPA. 2006. Photostasis and cold acclimation: Sensing low temperature through photosynthesis. Physiol Plantarum 126:28–44.

Folch J, Lees M, Stanley GHS. 1957. A simple method for the isolation and purification of total lipids from animal tissues. J Biol Chem 226:497–509.

Galland P, Pazur A. 2005. Magnetoreception in plants. J Plant Res 118:371–389.

Gantar M, Svirĉev V. 2008. Microalgae and cyanobacteria: Food for thought. J Phycol 44:260–268.

Griffiths DJ. 1970. The pyrenoid. Botanical Rev 36:29–58.

Grobbelaar J, Nedbal L, Tichý V. 1996. Influence of high frequency light/dark fluctuations on photosynthetic characteristics of microalgae photoacclimated to different light intensities and implications for mass algal cultivation. J Appl Phycol 8:335–343.

Hashish AH, El-Missiry MA, Abdelkader HI, Abou-Saleh RH. 2008. Assessment of biological changes of continuous whole body exposure to static magnetic field and extremely low frequency electromagnetic fields in mice. Ecotoxicol Environ Saf 71:895–902.

Hirano M, Ohta A, Abe K. 1998. Magnetic field effects on photosynthesis and growth of the cyanobacterium *Spirulina platensis*. J Ferment Bioeng 87:313–316.

Huner NPA, Öquist G, Melis A. 2003. Photostasis in plants, green algae and cyanobacteria: The role of light harvesting antenna complexes. In: Green BR, Parson WW, editors. Advances in photosynthesis, vol. 13, light harvesting antennas in photosynthesis. Boston, MA, USA: Kluwer Academic Publishers. pp 401–421.

Kirk JTO, Allen RL. 1965. Dependence of chloroplast pigment synthesis on protein synthesis: Effect of actidione. Biochem Biophys Res Commun 21:523–530.

Levin M, Ernst SG. 1995. Applied AC and DC magnetic fields cause alterations in the mitotic cycle of early sea urchin embryos. Bioelectromagnetics 16:231–240.

Li ZY, Guo SY, Li L, Cai MY. 2007. Effects of electromagnetic field on the batch cultivation and nutritional composition of *Spirulina platensis* in an air-lift photobioreactor. Biores Technol 98:700–705.

Mata TM, Martins AA, Caetano MS. 2010. Microalgae for biodiesel production and other applications: A review. Renew Sust Energ Rev 14:217–232.

Mecozzi M, Dragone P, Amici M, Peitrantonio E. 2000. Ultrasound assisted extraction and determination of the carbohydrate fraction in marine sediments. Org Geochem 31:1797–1803.

Meijer EA, Wijfels RH. 1998. Development of a fast, reproducible and effective method for extraction and quantification of proteins of micro-algae. Biotechnol Tech 12:353–358.

Metherel AH, Taha AY, Izadi H, Stark KD. 2009. The application of ultrasound energy to increase lipid extraction throughput of solid matrix samples (flaxseed). Prostaglandins Leukot Essent Fatty Acids 81:417–423.

Monde RA, Schuster G, Stern DB. 2000. Processing and degradation of chloroplast mRNA. Biochimie 82:573–582.

Pagliara P, Lanubile R, Dwikat M, Abbro L, Dini L. 2005. Differentiation of monocytic U937cells under static magnetic field exposure. Eur J Histochem 49:75–86.

Papazi A, Makridis P, Divanach P, Kotzabasis K. 2008. Bioenergetic changes in the microalgal photosynthetic apparatus by extremely high CO_2 concentrations induce an intense biomass production. Physiol Plant 132:338–349.

Potenza L, Ubaldi L, De Sanctis R, De Bellis R, Cucchiarini L, Dachà M. 2004. Effects of a static magnetic field on cell growth and gene expression in *Escherichia coli*. Mutat Res 561:53–62.

Pulz O, Gross W. 2004. Valuable products from biotechnology of microalgae. Appl Microbiol Biotechnol 65:635–648.

Repacholi MH, Greenebaum B. 1999. Interaction of static and extremely low frequency electric and magnetic fields with living systems: Health effects and research needs. Bioelectromagnetics 20:133–160.

Rosen AD, Chastney EE. 2009. Effect of long term exposure to 0.5 T static magnetic fields on growth and size of GH3cells. Bioelectromagnetics 30:114–119.

Sahebjamei H, Abdolmaleki P, Ghanati F. 2007. Effects of magnetic field on the antioxidant enzyme activities of suspension-cultured tobacco cells. Bioelectromagnetics 28: 42–47.

Stucki S, Vogel F, Ludwig C, Haiduc AG, Brandenberger M. 2009. Catalytic gasification of algae in supercritical water for biofuel production and carbon capture. Energy Environ Sci 2:535–541.

Tenuzzo B, Chionna A, Panzarini E, Lanubile R, Tarantino P, Di Jeso B, Dwikat M, Dini L. 2006. Biological effects of 6mT static magnetic fields: A comparative study in different cell types. Bioelectromagnetics 27:560–577.

Tran HL, Kwon JS, Kim ZH, Oh Y, Lee CG. 2010. Statistical optimization of culture media for growth and lipid production of *Botryococcus braunii* LB572. Biotechnol Bioprocess Eng 15:277–284.

Wang H-Y, Zeng X-B, Guo S-Y. 2007. Effects of magnetic treatment on ultrastructure of *Chlorella vulgaris*. Acta Laser Biol Sin 4:113–120.

Wang H-Y, Zeng X-B, Guo S-Y, Li Z-T. 2008. Effects of magnetic field on the antioxidant defense system of recirculation-cultured *Chlorella vulgaris*. Bioelectromagnetics 29:39–46.

Williams PJB, Laurens LML. 2010. Microalgae as biodiesel & biomass feedstocks: Review & analysis of the biochemistry, energetics & economics. Energy Environ Sci 3:554–590.

Woo DK, Shadel GS. 2011. Mitochondrial stress signals revise an old aging theory. Cell 144:11–12.

World Health Organization (WHO). 2006. Static Fields. Environmental Health Criteria 232. Geneva, Switzerland: World Health Organization.

Zech SG, Kurreck J, Eckert HJ, Renger G, Lubitz W, Bittl R. 1997. Pulsed EPR measurement of the distance between P680 and Qa in photosystem II. FEBS Lett 414:454–456.